Dissociation of Difluoroethylenes. I. Global Potential Energy Surface, RRKM, and VTST Calculations

Jesús González-Vázquez, Antonio Fernández-Ramos, Emilio Martínez-Núñez,* and Saulo A. Vázquez

Departamento de Química Física, Universidad de Santiago de Compostela, Santiago de Compostela, E-15706, Spain

Received: August 19, 2002

A global ground-state potential energy surface for the dissociation reactions of difluoroethylenes (DFEs) was computed by B3LYP and QCISD calculations, using the standard 6-311G(2d,2p) basis set. RRKM calculations were performed to compute relative abundances of hydrogen fluoride (HF) and molecular hydrogen produced from 1,1-DFE and from 1,2-DFE (cis and trans) at energies ranging from 110 to 180 kcal mol^{-1} relative to the zero point energy of 1,1-DFE. Thermal rate constants were also evaluated by the variational transition state theory for temperatures in the range 1250−1500 K. Both theoretical methods agree that, at the energies and temperatures studied, the main channel for HF elimination from 1,1-DFE is through a four-center transition state, whereas for 1,2-DFE the process occurs through a direct three-center elimination. At the energies studied, the RRKM method predicts that the main channel for molecular hydrogen elimination from the DFEs goes through a three-center transition state that connects 1,1-DFE with products.

Introduction

There has been considerable experimental and theoretical work devoted to characterizing the photodissociation dynamics of fluoroethylenes.[1−17] Several methods were used to excite the target molecules to energies at which molecular decomposition can take place. Pulsed ultraviolet light from a flash lamp or laser were often employed to promote excitation to a higher electronic state. The subsequent photofragmentation is expected to proceed primarily from a highly excited ground electronic state, formed by internal conversion or intersystem crossing from the initially excited electronic state. This is supported by the fact that similar results were obtained whether infrared multiphoton excitation[2] or Hg photosintetization[3,10] is used. Furthermore, the forms of the product translational energy distributions obtained for the photodissociation of fluoroethylenes also indicates that direct dissociation from the excited electronic state is unlikely.[12,13]

Among the unimolecular channels that can occur in fluoroethylenes, the molecular elimination of hydrogen fluoride (HF) is found to be the most important one. In vinyl fluoride, the simplest derivative, HF eliminations can be produced from a four-center or a three-center transition state. Sato et al.[6] investigated the photodissociation of vinyl fluoride by using mass-resolved photofragment time-of-flight spectroscopy. Additionally, they performed ab initio MP2/6-31G(d,p) calculations to provide further insights into the reaction mechanism of this system. Their calculations predicted classical barriers of 82.2 and 85.3 kcal mol^{-1} for the four-center and three-center eliminations. More recent calculations at the QCISD(T)/6-311G-(2d,2p) level afforded barriers of about 80 kcal mol^{-1} (74 kcal mol^{-1} including the zero point energy, ZPE) for both channels.[15] The reverse barriers for the four-center and three-center channels are, however, quite different: 52.2 and 9.3 kcal mol^{-1}, respectively, as calculated by QCISD(T)/6-311G(2d,2p). The differences between the three- and four-center transition states and between the associated exit barriers led Sato et al.[6] to conclude that HF is mainly produced through the four-center elimination channel. Recently, this conclusion was corroborated by a direct dynamics study in which the potential energy surface was computed by a semiempirical AM1 Hamiltonian modified by specific reaction parameters (AM1-SRP).[16]

For 1,1-difluoroethylene (1,1-DFE), only four-center HF eliminations can take place, assuming that 1,2 migration of H and F atoms is not facile. For 1,2-difluoroethylene (1,2-DFE), however, both the four- and three-center HF eliminations can occur. Watanabe et al.[3] reported vibrational distributions of HF produced by Hg-photosensitized reactions of fluoroethylenes. They found that for 1,1-DFE the fraction of the available energy that goes to HF vibration is much higher than the statistical one, whereas for 1,2-DFE the corresponding fraction is closer to that predicted by statistical calculations. Similarly, Lee and co-workers[12] found significant differences in the product translational energy distributions for HF elimination from 1,1-DFE and 1,2-DFE. As for vinyl fluoride, these discrepancies were attributed to differences in the exit barriers and transition states for the three- and four-center eliminations. In addition, they concluded that the three-center elimination is preferred in 1,2-DFE.[12] Product energy distributions for HF elimination from 1,1-DFE calculated by direct classical (and quasiclassical) trajectories[17] were found to be in good accord with experiment.

Apart from the HF elimination channel, Lee and co-workers[12] also observed eliminations of atomic and molecular hydrogen in the photodissociations of 1,1-DFE and 1,2-DFE at 193 nm. For 1,1-DFE at 157 nm, double bond braking and F atom elimination were also observed, but the branching ratio for the latter channel was found to be negligible.[13] At 193 nm of excitation, molecular hydrogen elimination is found to be more important for 1,1-DFE than for 1,2-DFE. This observation led Lee and co-workers[12] to conclude that, assuming that H and F atoms do not migrate, three-center H_2 elimination (from 1,1-DFE) is apparently preferred over four-center (from 1,2-DFE). Photolysis of 1,2-DFE produces some H_2/C_2F_2 that are faster

* Corresponding author. E-mail:uscqfemn@correo.cesga.es.

10.1021/jp021901s CCC: $25.00
Published on Web 02/07/2003

than those from 1,1-DFE, although the corresponding translational energy distributions are rather similar to each other; they peak at ~8 (1,1-DFE) and ~9 kcal mol^{-1} (1,2-DFE), indicating the presence of a small exit barrier.[12]

It is important to remark that the photodissociation studies of DFE were interpreted with the assumption that H and F migrations do not take place. Similarly, for the photodissociation of ethylene, the mechanism proposed in most investigations to explain the experimental data considered no appreciable hydrogen scrambling.[18−21] The comparison between the experimental data and results obtained by RRKM calculations (in which H scrambling was not considered) led Lee and coworkers[22−24] to conclude that the dissociation dynamics in ethylene may be nonstatistical in nature. By contrast, a recent classical trajectory study[25] suggests that hydrogen scrambling is significant and, furthermore, that the dissociation of ethylene occurs at, or near, the statistical limit if the process takes place in the electronic ground state. Therefore, it seems interesting to explore the possibility of H and F migrations in DFE in order to assess the importance of these processes in the global mechanism of the DFE photodissociation.

The pyrolysis of fluoroethylenes has also attracted the interest of experimentalists, although not as much as the photolysis. Simmie et al.[26,27] investigated the thermal decompositions of vinyl fluoride and 1,1-DFE in a single-pulse shock tube for the temperature ranges 1170−1350 K and 1287−1482 K, respectively. They found that the principal reaction is the unimolecular elimination of HF. Recently, da Silva et al.[28] reported ab initio and DFT calculations for the four-center elimination path of 1,1-DFE, as well as rate constants calculated by variational transition state theory. The calculated rates were found to be in agreement with those determined experimentally.

We thought it to be of interest to perform a theoretical investigation on the photolysis and pyrolysis of 1,1-DFE and 1,2-DFE in order to support and/or clarify the mechanism and main conclusions inferred from the experimental investigations. Our study is organized in two parts. The first part, which is presented in this paper, entails three main objectives: (1) a thorough characterization of the electronic ground-state potential energy surface (PES) for the fragmentation reactions of 1,1-DFE and 1,2-DFE, (2) an assessment of the relative importance of the molecular elimination processes at the excitation energies involved in the photodissociation studies, paying special attention to the possible implications of the H and F migrations, and (3) the evaluation of thermal rate constants for the HF elimination at temperatures at which successful pyrolysis of DFEs may take place. For these purposes, we employed high level ab initio and density functional theory (DFT) calculations,[29] RRKM calculations,[30] and variational transition state theory.[31] The second part of our study will involve the calculation, by using direct trajectories, of product energy partitioning for the HF elimination (the most important process) in the photodissociation of 1,2-DFE, which is presented in paper II.

Computational Details

Electronic Structure Calculations. Density functional and ab initio theories were employed to characterize the ground electronic potential energy surfaces for the fragmentation reactions of 1,1-DFE and 1,2-DFE. The DFT calculations were carried out with the B3LYP method and the 6-311G(2d,2p) standard basis set. This DFT method combines Becke's three-parameter nonlocal hybrid exchange potential[32,33] with the nonlocal correlation functional of Lee, Yang, and Parr.[34] Frequency calculations were then performed to characterize the stationary points as minima or saddle points and to evaluate zero point vibrational energies for the species investigated. In most cases, we followed the minimum energy path (MEP)[35,36] in order to either perform a subsequent VTST calculation or make sure that a transition structure connects with the expected reactant and product. The ab initio calculations involved quadratic CI optimizations including single and double substitutions (QCISD),[37] and, to obtain more accurate energies, QCISD-(T) single point energies (at the QCISD optimized geometries), that is, a triples contribution to the energy was added. All the electronic structure calculations were carried out using the GAUSSIAN 98 program package.[38]

RRKM Calculations. Microcanonical rate constants $k(E)$ were computed for 24 elementary steps involved in the HF and H_2 eliminations channels (see Appendix) using the well-known equation of the RRKM theory[30]

$$k(E) = \frac{\sigma W^{ts}(E)}{h\rho(E)} \tag{1}$$

where σ is the reaction path degeneracy, $W^{ts}(E)$ the total number of states at the transition state with energy less than or equal to E, and $\rho(E)$ the density of states at the reactant. In this work, $W^{ts}(E)$ and $\rho(E)$ were evaluated by direct count of vibrational states using a program[39] based on the Beyer−Swinehart algorithm.[40] The data employed in these calculations comprised the QCISD(T)//QCISD energy barriers and the B3LYP frequencies (for TS1−VII and TS1−VIII we used MP2 frequencies, and for *c*,*t*-TS we employed those obtained by CASSCF).

VTST Calculations. Thermal rate constants $k(T)$ were evaluated for all the HF elimination pathways shown in Figure 1. In all cases the MEP was followed at the B3LYP level of calculation, using the Page−McIver method[41] with a step size of 0.01 bohr and with Hessian calculations every 10 steps. This step size was small enough to provide convergent results of the thermal rate constants. As in the RRKM calculations, we correct the B3LYP barrier heights with the QCISD(T)//QCISD values.

Within the VTST,[31] we used the canonical variational transition state theory (CVT)[42] with small-curvature corrections for tunneling (SCT).[31,43] In this scheme, the CVT/SCT rate constant, $k^{CVT/SCT}(T)$, can be written as

$$k^{CVT/SCT}(T) = \kappa^{SCT}(T)k^{CVT}(T)$$

where $\kappa^{SCT}(T)$ is the SCT transmission factor for tunneling and $k^{CVT}(T)$ is the classical CVT rate constant, which is obtained by minimizing the generalized-transition-state rate constant along the MEP. All the CVT/SCT calculations were performed with GAUSSRATE 8.4,[44] which is an interface between the programs POLYRATE 8.9[45] and GAUSSIAN 98.[38]

Results and Discussion

Potential Energy Surface. The global ground-state potential energy profile obtained in this study for the dissociation channels of 1,1-DFE and 1,2-DFE is depicted in Figure 1. The numbers in this figure (and the energies reported in this section, unless otherwise stated) correspond to the electronic energies (in kcal mol^{-1}), relative to that of 1,1-DFE, calculated at the QCISD-(T)/6-311G(2d,2p)//QCISD/6-311G(2d,2p) level of theory. Figures 2−4 show the most relevant stationary points optimized with the QCISD method, along with their zero-point energy (ZPE) corrections obtained by B3LYP calculations, and for the transition states the imaginary frequency, too. Following is a description of the reaction paths comprising the global PES.

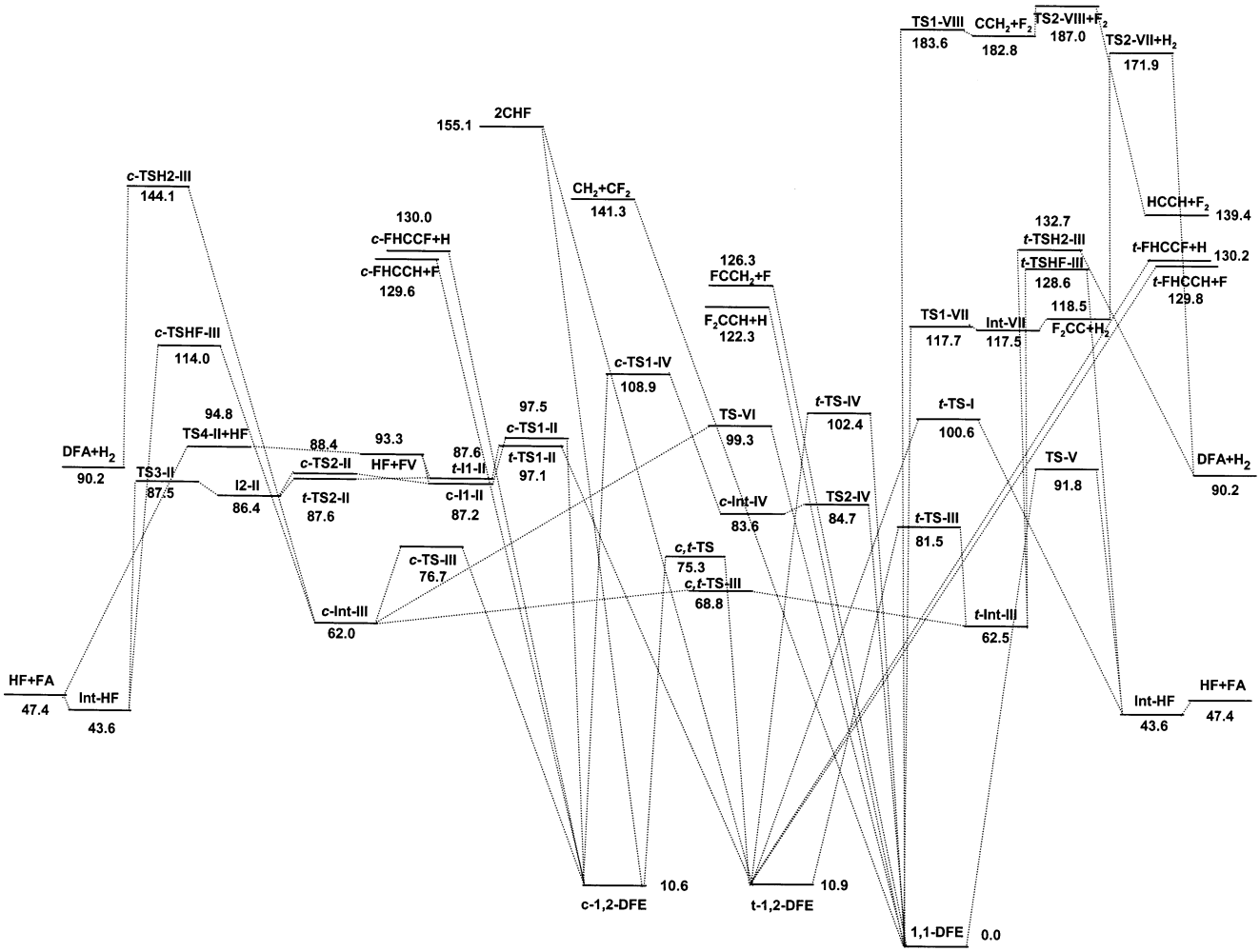

Figure 1. Schematic diagram of the ground electronic state global potential energy surface of difluoroethylenes. The relative energies were calculated at the QCISD(T)/6-311G(2d,2p)//QCISD/6-311G(2d,2p) level.

Channel I refers to the four-center HF elimination from *trans*-1,2-DFE. The associated transition state is referred to as *t*-TS-I, where the first (italic, lower case) letter (*t*) in this acronym indicates that this structure arises from the trans isomer of 1,2-DFE (*t*-1,2-DFE). The above transition state connects with a van der Waals (complex) minimum (Int-HF), which then dissociates to HF + fluoroacetylene (FA). Channels of type II refer to the three-center HF eliminations from both the cis and trans conformations of 1,2-DFE. As seen in Figure 1, these three-center HF elimination processes involve several elementary steps. The classical barrier (CB) for the first step is ∼86 kcal mol^{-1} in both cases, cis and trans, and the products are the van der Waals minima designated here as *c*-I1-II and *t*-I1-II, respectively. These two minima may dissociate directly to give HF + fluorovinylidene (FV), which then rearranges to form FA (via TS4-II), or, alternatively, those minima may evolve through transition states *c*-TS2-II and *t*-TS2-II to give a common van der Waals minimum, named as I2-II. This intermediate is then transformed to Int-HF (the FV → FA isomerization occurs in this step), which subsequently dissociates to HF + FA. Therefore, the elimination of HF and the isomerization of FV to FA takes place in a stepwise manner rather than in concert, which is in agreement with the suggestion of Lee and co-workers.[12]

As indicated in the Introduction, in this work we paid special attention to the possibility of H and F migrations. Channels of type III and IV in Figure 1 involve H and F migrations from 1,2-DFE, respectively. The structures for the relevant stationary points, together with the ZPE corrections and imaginary frequencies (for the transition states), are shown in Figure 3. Migration of a hydrogen atom in *cis*-1,2-DFE proceeds via transition state *c*-TS-III (CB = 66.1 kcal mol^{-1}) and produces an intermediate species (*c*-Int-III), which in turn may dissociate to give HF + FA (CB = 52.0 kcal mol^{-1}) or H_2 + difluoroacetylene (DFA, CB = 82.1 kcal mol^{-1}). The H atom migration from *trans*-1,2-DFE entails a similar profile. As seen in Figure 1, the relative energies for both intermediates (and those for *c*-TS-III and *t*-TS-III) are significantly lower than those for the transition states and intermediates of channels II and for *t*-TS-I (the transition state for the four-center HF elimination). However, the transition states for the last steps of channels of type III (especially those involving the elimination of molecular hydrogen) have relative energies substantially higher than those for channels I and II.

Migration of F atom from *cis*-1,2-DFE leads to intermediate *c*-Int-IV first (CB = 98.3 kcal mol^{-1}), and this in turn may evolve to 1,1-DFE. The two transition states involved in these two steps are named *c*-TS1-IV and *c*-TS2-IV. For *trans*-1,2-DFE, the B3LYP calculations predict two similar steps, with the first intermediate (*t*-Int-IV, not shown in the figure) having a HCCH dihedral angle of 40.6°. However, attempts to optimize this intermediate by QCISD calculations were unsuccessful. In particular, starting from the B3LYP geometry of *t*-Int-IV, the QCISD optimization led directly to 1,1-DFE.

Channels V−VIII initiate from 1,1-DFE. The relevant stationary points for the corresponding pathways are presented

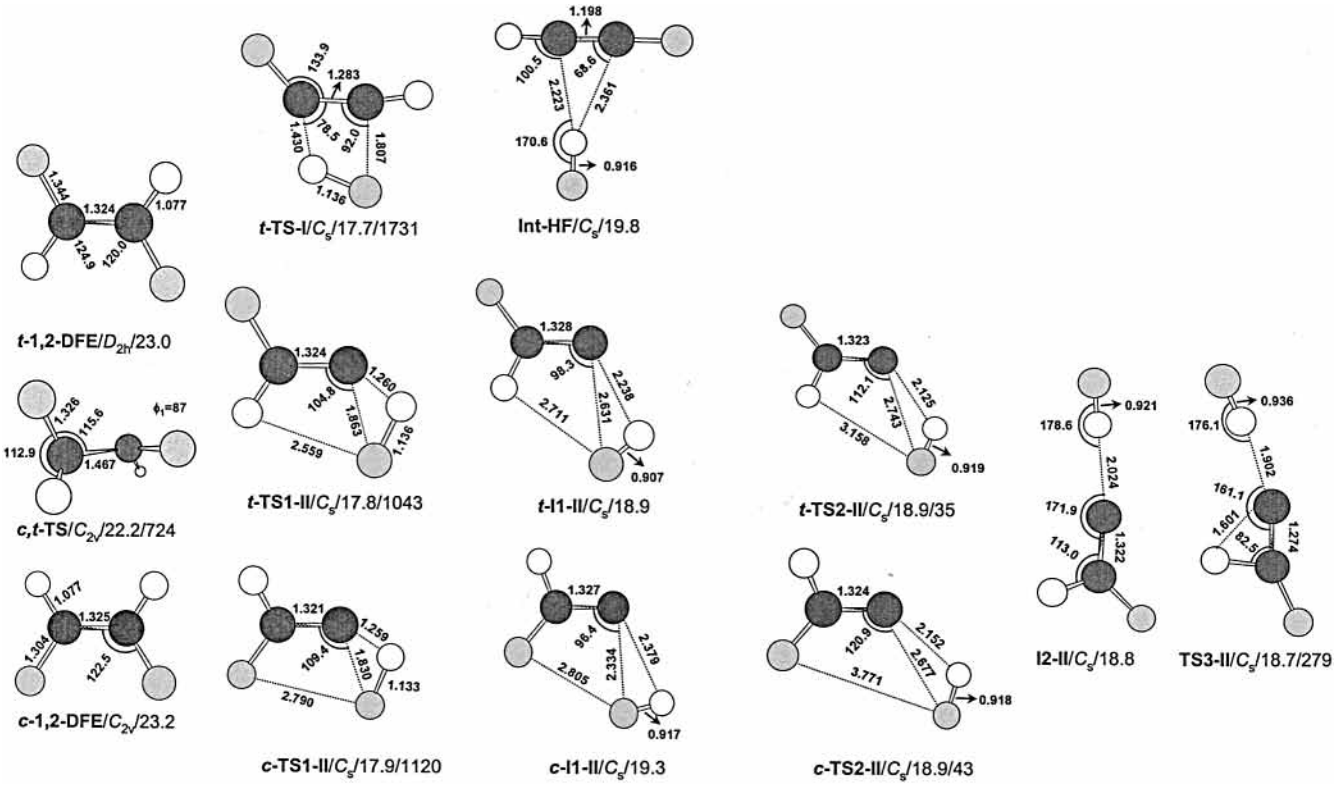

Figure 2. Main geometric parameters calculated at the QCISD/6-311G(2d,2p) level for the stationary points involved in channels I and II of 1,2-DFE (Int-HF and *c*,*t*-TS are shown here, although they are common to other channels). Below every structure are listed: the acronym used along the paper, the point-group symmetry, the ZPE evaluated at the B3LYP/6-311G(2d,2p) level in kcal mol^{-1}, and the imaginary frequency in cm^{-1} (only for transition states). For transition state *c*,*t*-TS, the geometries and ZPE were calculated at the CASSCF(2,2)/6-311G(2d,2p) level. In the structures, ϕ_1 and ϕ_2 refer to the FCCF and HCCH dihedral angles, respectively.

in Figure 4. Channel V is the four-center HF elimination from 1,1-DFE, which presents a classical barrier height (91.8 kcal mol^{-1}) similar to that for *trans*-1,2-DFE (89.7 kcal mol^{-1}). Fluorine migration from 1,1-DFE, referred to as channel VI in Figure 1, evolves via transition state TS-VI (99.3 kcal mol^{-1}), which connects with *c*-Int-III. Note that H migration from 1,1-DFE is related to channels IV, which were already detailed. Channel VII concerns the three-center H_2 elimination from 1,1-DFE. This pathway proceeds through TS1-VII (117.7 kcal mol^{-1}), and leads to a van der Waals minimum (Int-VII), which then dissociates to :C═CF_2 + H_2. The subsequent isomerization :C═CF_2 → FC≡CF (via TS2-VII) has a classical barrier height of 53.4 kcal mol^{-1}. Since the relative energy of TS2−VII + H_2 is very high (171.9 kcal mol^{-1}), this isomerization can only take place at very high excitation energies. This is in agreement with the result of Reiser et al.[46] in their infrared multiphoton excitation study of F_2C═CHCl that :C═CF_2 does not rearrange to form FC≡CF. On the other hand, the fact that the fastest translational energy for the H_2/C_2F_2 product from the 1,1-DFE photodissociation at 193 nm (∼40 kcal mol^{-1}) is significantly lower than that observed for 1,2-DFE (∼50 kcal mol^{-1}) led Balko et al.[12] to suggest that the above isomerization does not occur in concert with the three-center H_2 elimination (from 1,1-DFE), which is supported by our calculations.

The three-center elimination of molecular fluorine (channel VIII) to produce :C═CH_2 + F_2 first has a very large barrier height (183.6 kcal mol^{-1}), so that this channel is open only at very high energies. This explains why F_2 was not observed in the photodissociation studies of 1,1-DFE at 193 and 157 nm.[12,13] In the subsequent step of pathway VIII, vinylidene isomerizes to acetylene. We have to note that we could not find stationary points for TS1-VII and TS1-VIII by B3LYP calculations, although we optimized them with the QCISD and MP2 methods.

Figure 1 also shows direct atomic and C═C dissociations from 1,1-DFE and 1,2-DFE. Similar dissociations may also occur from the intermediates obtained in this study, but for clarity we have not depicted them in the figure. Atomic eliminations and C═C scissions were observed in the photodissociations of DFEs.[12,13] For 1,1-DFE at 157 nm excitation, H atom elimination becomes the second major dissociation pathway.[13]

Finally, we have to note that the cis−trans isomerization barrier for 1,2-DFE was calculated in this study at the CASSCF-(2,2)/6-311G(2d,2p) level, because the other quantum mechanical methods employed here do not describe appropriately the diradical character of the associated transition structure (denoted in Figure 1 by *c*,*t*-TS).[47] The barrier height obtained here, ∼65 kcal mol^{-1}, is similar to the experimental barrier for the related compound ethylene.[48]

Once the global PES has been detailed, it is worthwhile to remark the pathways leading to HF and H_2 eliminations. Hydrogen fluoride may be eliminated from channels I, II (cis and trans), III (cis and trans), and V, independently on whether the reactant is 1,1-DFE or 1,2-DFE because both isomers are connected between each other, as shown in Figure 1. On the other hand, H_2 may be eliminated through channels III (cis and trans) and VII. Notice that we have not found a transition state for a direct four-center H_2 elimination from *trans*-1,2-DFE; neither for vinyl fluoride[6,15] nor for ethylene[21,22] was a transition state of that kind achieved. Our mechanism, therefore, is much more involved than that inferred from previous photodissociation studies, and may help to understand more clearly the experimental observations. For instance, Lee and co-workers[12,13] assumed that H and F migration (in the excited electronic state) is negligible. Here we find that, in principle, these processes may occur on the electronic ground state. In the next section,

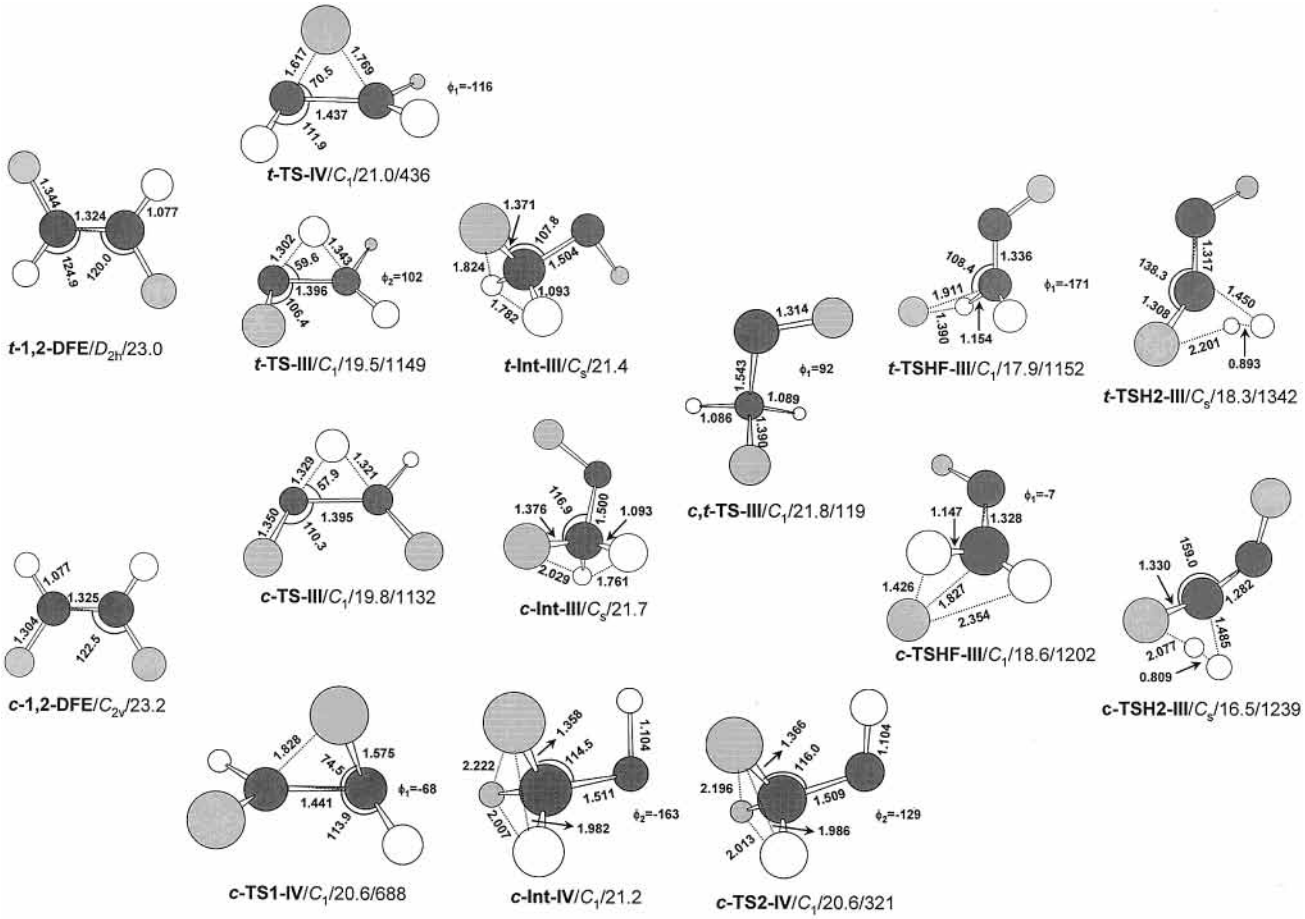

Figure 3. Same as Figure 2, but for channels III and IV.

we will show that H migration has significant implications as far as the H_2 elimination from 1,2-DFE is concerned.

RRKM Calculations. Micocanonical rate constants for energies ranging from 110 to 180 kcal mol^{-1} (above the ZPE of 1,1-DFE) were computed for HF and H_2 eliminations using the RRKM theory. The rate constants were then employed to evaluate relative abundances of H_2 and F_2 as a function of the energy and for every reaction pathway. The rate equations for the molecular elimination channels are shown in the Appendix. A compilation of the energies, geometries, and frequencies used in the RRKM calculations is included as Supporting Information. The relative abundances obtained in this work for 1,1-DFE as reactant are displayed graphically in Figure 5. At the lowest energies investigated, the four-center HF elimination from 1,1-DFE (channel V) dominates the dissociation completely. As energy increases, H_2 elimination, via channel VII only (the three-center elimination from 1,1-DFE), becomes significant and competes with the above HF pathway (channel V). The other molecular elimination channels are insignificant at the energies studied. Therefore, for 1,1-DFE our results are in agreement, at least qualitatively, with the experimental observations[12,13] and conform with the basic mechanism used to interpret the experimental data. At 157 nm, however, the HF/H_2 experimental ratio (~4.7) is substantially higher than that predicted here (~1.2). It should be noticed that at this energy the actual rates might be controlled by the intramolecular vibrational energy redistribution, and so the applicability of the statistical RRKM theory is limited.

The relative abundances of H_2 and HF obtained here for 1,2-DFE (we assumed equal amounts of cis and trans isomers) are shown in Figure 6. The calculations show that the HF elimination (as a whole) is the dominant process in the energy range studied, and that the three-center eliminations from 1,2-DFE (channels II) are favored over the four-center elimination from *trans*-1,2-DFE, in agreement with the conclusion of Balko et al.[12] As the energy increases the elimination of H_2 becomes significant, although in this case the percentage is quite small, which agrees with the experimental observation that the H_2 elimination is more important in 1,1-DFE than in 1,2-DFE.[12] Balko et al.[12] considered that H_2 is produced only via four-center elimination in the photolysis of 1,2-DFE, and, on account of the relative translational energies, they suggested that the reverse barrier for that channel should be small (similar to that for the three-center H_2 elimination from 1,1-DFE). Obviously, from the experimental data obtained in their study, their interpretation appears to be very reasonable. However, our investigation predicts a very different mechanism for molecular hydrogen elimination. Apart from the fact that we have not found a direct four-center H_2 elimination mechanism from 1,2-DFE, our results predict that the most important pathway for H_2 elimination involves H and F migration (see Figure 6), that is, 1,1-DFE is formed first, and then H_2 is eliminated by the three-center, channel VII. Another significant pathway for H_2 elimination involves H migration to give *t*-Int-III, with its subsequent dissociation via *t*-TSH2-III. The exit barrier for channel VII is virtually negligible, and that for H_2 elimination through *t*-TSH2−III is quite large (46.0 kcal mol^{-1} with the zero-point energy corrections). Thus, our mechanism may explain why the $H_2 + C_2F_2$ translational distributions are so similar for 1,1-DFE and 1,2-DFE (peaking at ~8 and ~9 kcal mol^{-1}, respectively), and why some of the H_2/C_2F_2 produced in the photolysis are faster for the latter than for the former.

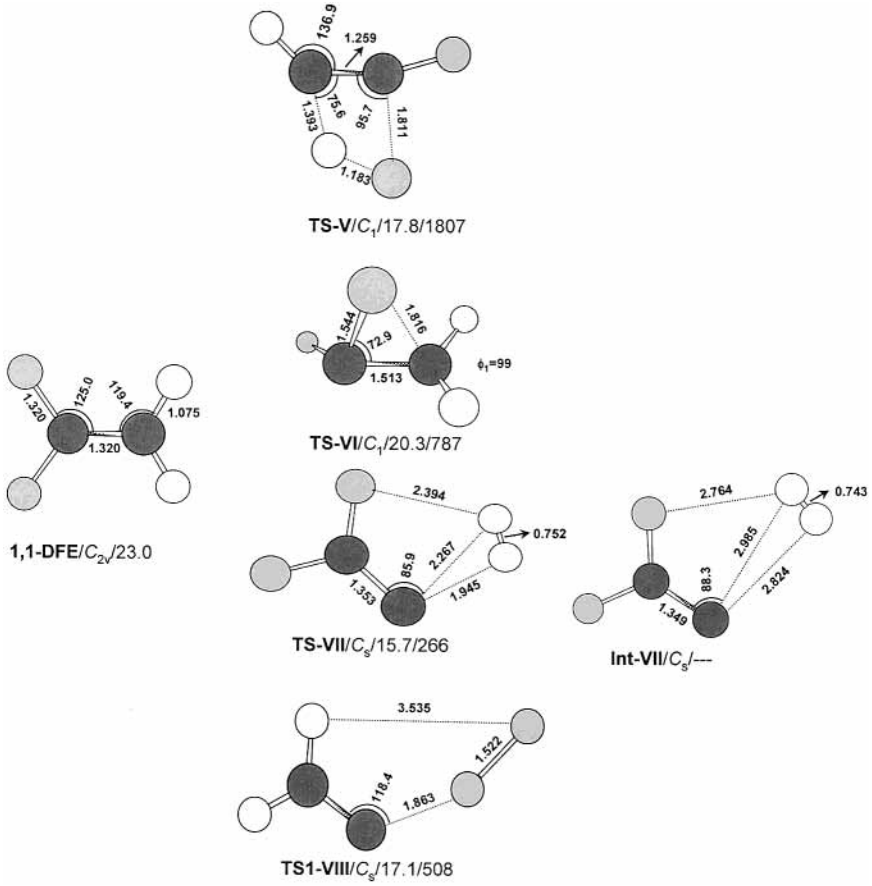

Figure 4. Same as Figure 2, but for channels V to VIII. For stationary points TS-VII and TS1-VIII, the ZPE corrections were evaluated at the MP2/6-31G(d,p) and MP2/6-311G(2d,2p) levels, respectively.

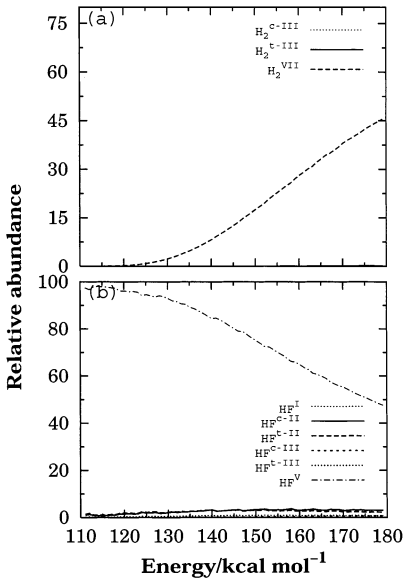

Figure 5. Relative abundances obtained by the RRKM method for (a) H_2 and (b) HF in the energy range 110−180 kcal mol^{-1}, which are produced from the photodissociation of 1,1-DFE.

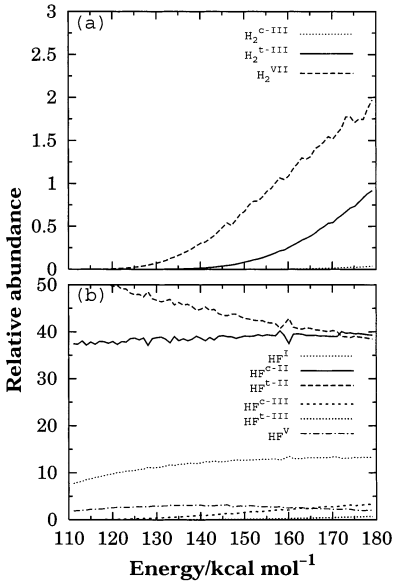

Figure 6. Same as Figure 5 but for 1,2-DFE.

Thermal Rate Constants. The $k^{CVT/SCT}(T)$ rate constants were evaluated by dual-level direct dynamics, specifically by following the MEP at the B3LYP level (low level) with interpolated optimized single point energies (ISPE)[49] at the stationary points at the QCISD(T)/QCISD level (high level). In this paper we used the simplest form of ISPE in which the high-level energies along the MEP are obtained by interpolation based on the supply of high-level energies only at the stationary points. For the HF elimination reactions this dual-level correction suffices because both the variational and tunneling contributions to the rate constant are expected to be small, and the major effect due to change in the barrier height is taken into account. Thus, the rate constants obtained by the CVT/SCT method are quite close to those obtained by the conventional transition state theory (TST).

The CVT/SCT thermal rate constants obtained in this work for the four-center HF elimination from 1,1-DFE (for temperatures ranging from 1250 to 1500 K) are compared with the

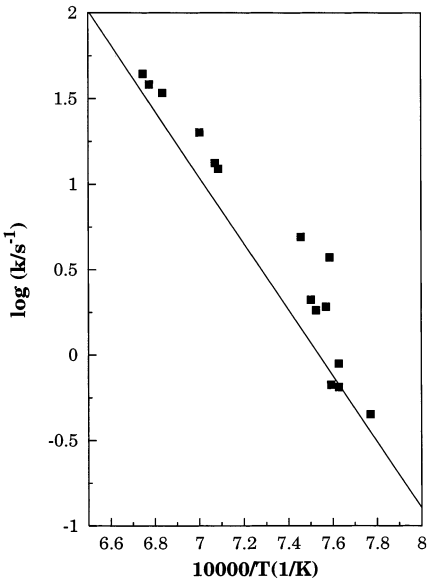

Figure 7. Arrhenius plot showing the calculated CVT/SCT thermal rate constants for the four-center HF elimination from 1,1-DFE (solid line) together with the experimental values of ref 27 (squares).

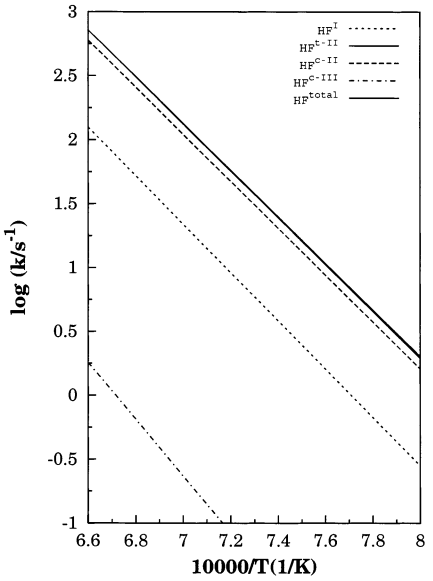

Figure 8. Arrhenius plot showing the calculated CVT/SCT thermal rate constants for the HF elimination from 1,2-DFE through channels I, II, and III. The total and *t*-II rate constants have very similar values and appear superimposed in the graph.

available experimental data in Figure 7. The thermal rate constants for the other possible channels of HF elimination were not evaluated because, as shown in the previous section, the RRKM calculations predicted negligible contributions. As can be seen, the agreement between the theoretical and experimental rates is good. The calculated activation energy in the temperature range studied is 88.6 kcal mol^{-1}, a value within the experimental error of the measured value (86 $\pm$ 7 kcal mol^{-1}).

Figure 8 plots the thermal rate constants calculated for 1,2-DFE at temperatures in the range 1250−1500 K. In this case, no experimental information is available; however, we are quite confident of the accuracy of these calculations, seeing that for 1,1-DFE good agreement between theory and experiment was achieved. For the sake of simplicity, channel V was not considered in these calculations, but the contribution of this channel should be negligible, taking the RRKM results into account. Actually, the total rate constant for HF elimination almost coincides with that obtained for channel *t*-II, with a small contribution from *c*-II. Therefore, we conclude that direct three-center HF eliminations dominate over the other possible channels.

Conclusions

The potential energy profile calculated in this work predicts several pathways for HF and H_2 eliminations. There are six possible mechanisms for HF elimination and three for H_2 elimination. For HF elimination we found the four-center elimination from *trans*-1,2-DFE (channel I), the three-center elimination from cis and trans 1,2-DFE (channels *c*-II and *t*-II), the three-center elimination from *c*-Int-III and *t*-Int-III (through transition states *c*-TSHF-III and *t*-TSHF-III, respectively), and the four-center elimination from 1,1-DFE (channel V). The three possible mechanisms for H_2 elimination are the three-center elimination from *c*-Int-III and *t*-Int-III (through transition states *c*-TSH2-III and *t*-TSH2-III, respectively), and the three-center elimination from 1,1-DFE. All these are open channels at 193 and 157 nm of excitation, either if the reactant is 1,1-DFE or 1,2-DFE because they are connected through H and F migrations.

The RRKM calculations predict that the HF elimination is the dominant process for the DFE dissociations. For 1,1-DFE, the HF elimination occurs by the direct four-center mechanism (channel V). The contributions from other pathways are insignificant. For 1,2-DFE, the three-center eliminations through channels II are the most important processes. Therefore, as far as the HF elimination is concerned, the calculations support the mechanisms considered in the experimental investigations. The elimination of H_2 from 1,1-DFE and 1,2-DFE mainly occurs through a direct three-center elimination from 1,1-DFE. A direct four-center mechanism for H_2 elimination was not found.

Acknowledgment. E.M.-N. and S.A.V. thank Ministerio de Ciencia y Tecnología of Spain for financial support (Project BQU2000-0462). E.M.-N. and A.F.-R. also thank the above Ministry for their Ramón y Cajal research contracts.

Appendix: DFEs Rate Equations

Proposed mechanism for the HF, H_2, and F_2 photodissociation reactions:

$$t-1,2-\mathrm{DFE}\begin{cases} \xrightarrow{k_1} \mathrm{FA}+\mathrm{HF}^{\mathrm{I}} \\ \xrightarrow{k_{2,t}} \mathrm{FA}+\mathrm{HF}^{t-\mathrm{II}} \\ \underset{k_{-3,t}}{\overset{k_{3,t}}{\rightleftarrows}} t\text{-Int-III} \\ \underset{k_{-4,t}}{\overset{k_{4,t}}{\rightleftarrows}} 1,1-\mathrm{DFE} \end{cases} \qquad c-1,2-\mathrm{DFE}\begin{cases} \xrightarrow{k_{2,c}} \mathrm{FA}+\mathrm{HF}^{c-\mathrm{II}} \\ \underset{k_{-3,c}}{\overset{k_{3,c}}{\rightleftarrows}} c-\mathrm{Int}-\mathrm{III} \\ \underset{k_{-4,c}}{\overset{k_{4,c}}{\rightleftarrows}} 1,1-\mathrm{DFE} \\ \underset{k_{-9}}{\overset{k_{9}}{\rightleftarrows}} t-1,2-\mathrm{DFE} \end{cases}$$

$$1,1-\mathrm{DFE}\begin{cases} \xrightarrow{k_5} \mathrm{FA}+\mathrm{HF}^{\mathrm{V}} \\ \underset{k_{-6}}{\overset{k_{6}}{\rightleftarrows}} c-\mathrm{Int}-\mathrm{III} \\ \xrightarrow{k_7} \mathrm{DFA}+\mathrm{H}_2^{\mathrm{VII}} \\ \xrightarrow{k_8} \mathrm{HCCH}+\mathrm{F}_2 \end{cases} \qquad t-\mathrm{Int}-\mathrm{III}\begin{cases} \xrightarrow{k_{10}} \mathrm{FA}+\mathrm{HF}^{,t-\mathrm{III}} \\ \xrightarrow{k_{11}} \mathrm{DFA}+\mathrm{H}_2^{t-\mathrm{III}} \\ \underset{k_{-14}}{\overset{k_{14}}{\rightleftarrows}} c-\mathrm{Int}-\mathrm{III} \end{cases}$$

$$c-\mathrm{Int}-\mathrm{III}\begin{cases} \xrightarrow{k_{12}} \mathrm{DFA}+\mathrm{HF}^{c-\mathrm{III}} \\ \xrightarrow{k_{13}} \mathrm{FA}+\mathrm{H}_2^{c-\mathrm{III}} \end{cases}$$

In the above scheme we considered that 1,1-DFE leads directly to *c*-1,2-DFE (and vice versa), which is a reasonable approximation because the stability of the *c*-Int-IV intermediate is only of 0.5 kcal/mol after ZPE correction. This scheme leads to the following kinetic equations, which, expressed as a system of ordinary differential equations (ODEs) of the type $d\vec{x}/dt = A\vec{x}$, is given by:

$$\begin{pmatrix} \mathrm{d[1,1\text{-}DFE]/dt} \\ \mathrm{d[}c\text{-1,2-DFE]/dt} \\ \mathrm{d[}t\text{-1,2-DFE]/dt} \\ \mathrm{d[}c\text{-Int-III]/dt} \\ \mathrm{d[}t\text{-Int-III]/dt} \end{pmatrix} = \begin{pmatrix} -\alpha_1 & k_{4,c} & k_{4,t} & k_{-6} & 0 \\ k_{-4,c} & -\alpha_2 & k_{-9} & k_{-3,c} & 0 \\ k_{-4,t} & k_9 & -\alpha_3 & 0 & k_{-3,t} \\ k_6 & k_{3,c} & 0 & -\alpha_4 & k_{-14} \\ 0 & 0 & k_{3,t} & k_{14} & -\alpha_5 \end{pmatrix} \begin{pmatrix} \mathrm{[1,1\text{-}DFE]} \\ \mathrm{[}c\text{-1,2-DFE]} \\ \mathrm{[}t\text{-1,2-DFE]} \\ \mathrm{[}c\text{-Int-III]} \\ \mathrm{[}t\text{-Int-III]} \end{pmatrix} \quad \text{(A.1)}$$

where

$$\alpha_1 = k_{-4,c} + k_{-4,t} + k_5 + k_6 + k_7 + k_8$$

$$\alpha_2 = k_{2,c} + k_{3,c} + k_{4,c} + k_9$$

$$\alpha_3 = k_1 + k_{2,t} + k_{3,t} + k_{4,t} + k_{-9}$$

$$\alpha_4 = k_{-3,c} + k_{-6} + k_{12} + k_{13} + k_{14}$$

$$\alpha_5 = k_{-3,t} + k_{10} + k_{11} + k_{-14}$$

The solution of this system of ODEs is of the type

$$x_j = \sum_{i=1}^{5} c_i \exp(\lambda_i t)\, u_{ij} \quad \text{(A.2)}$$

x_j being the concentrations of the reactive species, λ_i and **u** the eigenvalues and eigenvectors of the *A* matrix, respectively. The constants, c_i, are obtained from the initial conditions. Subsequently, the solutions of the system are used to get the concentrations of HF, H_2, and F_2 at $t \rightarrow \infty$ of the different channels from the integration of the following rate equations:

$$\frac{\mathrm{d[HF^{I}]}}{\mathrm{dt}} = k_1[t\text{-1,2-DFE}] \quad \text{(A.3)}$$

$$\frac{\mathrm{d[HF^{II,}}^{t}\mathrm{]}}{\mathrm{dt}} = k_{2,t}[t\text{-1,2-DFE}] \quad \text{(A.4)}$$

$$\frac{\mathrm{d[HF^{II,}}^{c}\mathrm{]}}{\mathrm{dt}} = k_{2,c}[c\text{-1,2-DFE}] \quad \text{(A.5)}$$

$$\frac{\mathrm{d[HF^{III,}}^{c}\mathrm{]}}{\mathrm{dt}} = k_{12}[t\text{-Int-III}] \quad \text{(A.6)}$$

$$\frac{\mathrm{d[HF^{III,}}^{t}\mathrm{]}}{\mathrm{dt}} = k_{10}[t\text{-Int-III}] \quad \text{(A.7)}$$

$$\frac{\mathrm{d[HF^{V}]}}{\mathrm{dt}} = k_5[1,1\text{-DFE}] \quad \text{(A.8)}$$

$$\frac{\mathrm{d[H_2^{III,}}^{t}\mathrm{]}}{\mathrm{dt}} = k_{11}[t\text{-Int-III}] \quad \text{(A.9)}$$

$$\frac{\mathrm{d[H_2^{III,}}^{c}\mathrm{]}}{\mathrm{dt}} = k_{13}[c\text{-Int-III}] \quad \text{(A.10)}$$

$$\frac{\mathrm{d[H_2^{VII}]}}{\mathrm{dt}} = k_7[1,1\text{-DFE}] \quad \text{(A.11)}$$

$$\frac{\mathrm{d[F_2]}}{\mathrm{dt}} = k_8[1,1\text{-DFE}] \quad \text{(A.12)}$$

Supporting Information Available: Structural parameters at different levels of theory of the stationary points needed in the RRKM calculations. This material is available free of charge via the Internet at http://pubs.acs.org.

References and Notes

(1) Berry, M. J.; Pimentel, G. C. *J. Chem. Phys.* **1969**, *51*, 2274.
(2) Quick, C. R., Jr.; Wittig, C. *J. Chem. Phys.* **1980**, *72*, 1694.
(3) Watanabe, H.; Horiguchi, H.; Tsuchiya, S. *Bull. Chem. Soc. Jpn.* **1980**, *53*, 1530.
(4) Donaldson, D. J.; Watson, D. G.; Sloan, J. *J. Chem. Phys.* **1982**, *68*, 95.
(5) Kato, S.; Morokuma, K. *J. Chem. Phys.* **1980**, *74*, 6285.
(6) Sato, K.; Tsunashima, S.; Takayanagi, T.; Fijisawa, G.; Yokoyama, A. *Chem. Phys. Lett.* **1995**, *242*, 401.
(7) Takayanagi, T.; Yokoyama, A. *Bull. Chem. Soc. Jpn.* **1995**, *68*, 2245.
(8) Lin, S.-R.; Lin, S.-C.; Lee, Y.-C.; Chou, Y.-C.; Chen, I.-C.; Lee, Y.-P. *J. Chem. Phys.* **2000**, *114*, 7396.
(9) Strausz, P. O.; Norstrom, R. J.; Salahub, D.; Gosavi, R. K.; Gunning, H. E.; Csizmadia, I. G. *J. Am. Chem. Soc.* **1970**, *92*, 6395.
(10) Clough, P. N.; Polanyi, J. C.; Taguchi, R. T. *Can. J. Chem.* **1970**, *48*, 2919.
(11) Hall, G. E.; Muchermann, J. T.; Presses, J. M.; Weston, R. E., Jr.; Flynn, G. W.; Persky, A. *J. Chem. Phys.* **1994**, *101*, 3679.
(12) Balko, B. A.; Zhang, J.; Lee, Y. T. *J. Phys. Chem. A* **1997**, *101*, 6611.
(13) Lin, J. J.; Wu, S. M.; Huang, D. W.; Lee, Y. T.; Yang, X. *J. Chem. Phys.* **1998**, *109*, 10838.
(14) Lin, S.-R.; Lee, Y.-P. *J. Chem. Phys.* **1999**, *111*, 9233.
(15) Martínez-Núñez, E.; Vázquez, S. A. *Struct. Chem.* **2001**, *12*, 95.
(16) Martínez-Núñez, E.; Vázquez, S. A. *Chem. Phys. Lett.* **2000**, *332*, 583.
(17) Martínez-Núñez, E.; Estévez, C. M.; Flores, J. R.; Vázquez, S. A. *Chem. Phys. Lett.* **2001**, *348*, 81.
(18) Okabe, H.; McNesby, J. R. *J. Chem. Phys.* **1962**, *36*, 601.
(19) Balko, B. A.; Zhang, J.; Lee, Y. T. *J. Chem. Phys.* **1992**, *97*, 935.
(20) Stolow, A.; Balko, B. A.; Cromwell, E. F.; Zhang, J.; Lee, Y. T. *J. Photochem. Photobiol. A* **1992**, *62*, 285.
(21) Chang, A. H. H.; Mebel, A. M.; Yang, X.-M.; Lin, S. H.; Lee, Y. T. *Chem. Phys. Lett.* **1998**, *287*, 301.
(22) Chang, A. H. H.; Mebel, A. M.; Yang, X.-M.; Lin, S. H.; Lee, Y. T. *J. Chem. Phys.* **1998**, *109*, 2748.
(23) Cromwell, E. F.; Stolow, A.; Vrakking, M. J. J.; Lee, Y. T. *J. Chem. Phys.* **1992**, *97*, 4029.
(24) Chang, A. H. H.; Hwang, D. W.; Yang, X.-M.; Mebel, A. M.; Lin, S. H.; Lee, Y. T. *J. Chem. Phys.* **1999**, *110*, 10810.
(25) Peña-Gallego, A.; Martínez-Núñez, E.; Vázquez, S. A. *Chem. Phys. Lett.* **2002**, *353*, 418.
(26) Simmie, J. M.; Quiring, W. J.; Tschuikow-Roux, E. *J. Phys. Chem.* **1970**, *74*, 992.
(27) Simmie, J. M.; Tschuikow-Roux, E. *J. Phys. Chem.* **1970**, *74*, 4075.
(28) da Silva, A. M.; Arbilla, G.; da Silva, E. C. *J. Phys. Chem. A* **2000**, *104*, 9535.
(29) Jensen, F. *Introduction to Computational Chemistry*; John Wiley & Sons: New York, 1999.
(30) Forst, W. *Theory of Unimolecular Reactions*; Academic: New York, 1973.
(31) Truhlar, D. G.; Isaacson, A. D.; Garrett, B. C. In *Theory of Chemical Reaction Dynamics*; Baer, M., Ed.; CRC Press: Boca Raton, FL, 1985; p 65.
(32) Becke, A. D. *J. Chem. Phys.* **1993**, *98*, 5648.
(33) Becke, A. D. *J. Chem. Phys.* **1992**, *96*, 2155.
(34) Lee, C.; Yang, W.; Parr, R. G. *Phys. Rev.* **1988**, *B37*, 785.
(35) Fukui, K. *J. Phys. Chem.* **1970**, *74*, 4161.
(36) Gonzalez, C.; Schlegel, H. B. *J. Chem. Phys.* **1989**, *90*, 2154.
(37) Pople, J. A.; Head-Gordon, M.; Raghavachari, K. *J. Chem. Phys.* **1987**, *87*, 5968.

(38) Frisch, M. J.; Trucks, G. W.; Schlegel, H. B.; Scuseria, G. E.; Robb, M. A.; Cheeseman, J. R.; Zakrzewski, V. G.; Montgomery, J. A.; Stratmann, R. E.; Burant, J. C.; Dapprich, S.; Millam, J. M.; Daniels, A. D.; Kudin, K. N.; Strain, M. C.; Farkas, O.; Tomasi, J.; Barone, V.; Cossi, M.; Cammi, R.; Mennucci, B.; Pomelli, C.; Adamo, C.; Clifford, S.; Ochterski, J.; Petersson, G. A.; Ayala, P. Y.; Cui, Q.; Morokuma, K.; Malick, D. K.; Rabuck, A. D.; Raghavachari, K.; Foresman, J. B.; Cioslowski, J.; Ortiz, J. V.; Stefanov, B. B.; Liu, G.; Liashenko, A.; Piskorz, P.; Komaromi, I.; Gomperts, R.; Martin, R. L.; Fox, D. J.; Keith, T.; Al-Laham, M. A.; Peng, C. Y.; Nanayakkara, A.; Gonzalez, C.; Challacombe, M.; Gill, W. P. M.; Johnson, B. G.; Chen, W.; Wong, M. W.; Andres, J. L.; Head-Gordon, M.; Replogle E. S.; Pople, J. A. Gaussian 98 Revision A.7, Gaussian, Inc.: Pittsburgh, PA, 1998.

(39) Martínez-Núñez, E., unpublished work.

(40) Beyer, T.; Swinehart, D. R. *ACM Commun*. **1973**, *16*, 379.

(41) Page, M.; McIver, J. W. *J. Chem. Phys.* **1988**, *88*, 922.

(42) Garrett, B. C.; Truhlar, D. G. *J. Phys. Chem.* **1979**, *83*, 1053.

(43) Liu, Y.-P.; Lynch, G. C.; Truong, T. N.; Lu, D.-h.; Truhlar, D. G.; Garrett, B. C. *J. Am. Chem. Soc.* **1993**, *115*, 7806.

(44) Corchado, J. C.; Chuang, Y.-Y.; Coitiño, E. L.; Truhlar, D. G. *GAUSSRATE* versión 8.4; University of Minnesota; Minneapolis, MN, 1999.

(45) Corchado, J. C.; Chuang Y.-Y.; Fast, P. L.; Villà, J.; Hu, W.-P.; Liu, Y.-P.; Lynch, G. C.; Nguyen, K. A.; Jackels, C. F.; Melissas, V. S.; Lynch, B. J.; Rossi, I.; Coitiño, E. L.; Fernández-Ramos, A.; Pu, J.; Albu, T. V.; Steckler, R.; Garret, B. C.; Isaacson, A.; Truhlar, D. G. *POLYRATE* version 8.9; University of Minnesota, Minneapolis, MN, 2002.

(46) Reiser, C.; Steinfeld, J. I. *J. Phys. Chem.* **1980**, *84*, 681.

(47) Krylov, A.; Sherrill, C. D.; Byrd, E. F. C.; Head-Gordon, M. *J. Chem. Phys.* **1998**, *109*, 10669.

(48) Douglas, J. E.; Rabinovitch, B. S.; Looney, F. S. *J. Chem. Phys.* **1955**, *23*, 315.

(49) Chuang, Y.-Y.; Corchado, J. C.; Truhlar, D. G. *J. Phys. Chem. A* **2000**, *103*, 1140.